ISSN 1330-3651 (Print), ISSN 1848-6339 (Online)
DOI: 10.17559/TV-20161115224752

THERMAL MODEL OF THROUGH FLOW UNIVERSAL MOTOR BY MEANS OF LUMPED PARAMETER NETWORK

Blaž Benedik, Jože Duhovnik, Janez Rihtaršič, Jože Tavčar

Original scientific paper
Being able to predict temperature rise inside a machine is as important as predicting its performance and life. Because temperature measurements and computational thermal simulations can be time consuming, thermal paths inside the through-flow universal motor were described by means of simple lumped parameter thermal network. Once the model was built, its unknown convection coefficients were tuned with the genetic algorithm tool in MatLab. The model has been applied and successfully verified with measurements on two different types of a vacuum cleaner motor. Taking account of impeller losses as one of the model inputs makes temperature estimates more accurate regardless of machine's operational regime.

Keywords: *genetic algorithm; lumped parameter network; open-circuit cooling; steady-state thermal model; universal motor; vacuum cleaner motor*

Toplinski model protočnog univerzalnog motora pomoću mreže skupnog parametra

Izvorni znanstveni članak
Biti u stanju predvidjeti porast temperature unutar stroja jednako je važno kao i predvidjeti njegovo djelovanje i radni vijek. Budući da mjerenja temperature i toplinske simulacije računalom mogu zahtijevati puno vremena, putovi topline unutar protočnog univerzalnog motora su opisani jednostavnom toplinskom mrežom skupnog (lumped) parametra. Jednom kad je model izgrađen, njegovi nepoznati koeficijenti konvekcije su usklađeni s alatom genetičkog algoritma u MatLab. Model je primijenjen i uspješno provjeren mjerenjima na dva različita tipa motora usisivača za prašinu. Uzimajući u obzir gibitke rotora kao jednog od ulaza modela, procjene temperature su točnije bez obzira na radni režim stroja.

Ključne riječi: *genetski algoritam; hlađenje otvorenog strujnog kruga; motor usisivača za prašinu; mreža skupnog parametra; toplinski model stacionarnog stanja; univerzalni motor*

1 Introduction

With requirements to use less material for products and at the same time gain their efficiency, there is a need to exploit materials to their limits. This is the reason why thermal analysis of electric machines gained on its importance and is receiving more attention of academic research and industrial use. It has now become necessary to analyse thermal behaviour of machines to the same extent as exploration of their electromagnetic aspects.

In the development of electric machines in general, and universal motors in particular, temperature rise is a key factor affecting the efficiency of the motor and the life span of its vital components such as bearings, impregnated windings and carbon brushes. Thermal data allow estimating surveillance, protection and operational limits of the machine.

Thermal models based on different numerical techniques, such as finite difference or finite element method are available now. However, the accuracy of used method is still limited by input parameters no matter how refined the discretization. To consider axial heat flow, a 3-diminsional model is required, while the influence of forced air ventilation requires complex computational fluid dynamic (CFD) simulations, which both make numerical techniques expensive to run. Therefore, due to its simplicity, lumped parameter network is more attractive as it relatively accurately describes thermal conditions within the machine elements [1-7].

Recent introduction of energy labels into vacuum cleaner appliance market brought significant market changes also for manufacturers of vacuum cleaner motors. In a relatively short period of time there were two energy regulations introduced on EU markets. In 2014 the max allowed electric power of a vacuum cleaner appliance was limited to 1600 W and in 2017 this limit will be further reduced to 900 W. Not just performance and price, but also time necessary to introduce modifications grew in importance. Even small design adjustments, such as modified winding data or a revised type of bearings, brushes, impeller, etc. can cause significant temperature shifts within some of the components.

Furthermore, by customer-focused development, such design adjustments occur frequently during the development process. In case of using numerical technics, even minor design adoptions would require another computational run for gaining new temperature data.

The most important reasons why thermal modelling of vacuum cleaner motor as a type of through flow universal motor should be dealt with separately from other induction machines, have already been described in our previous work [8], while two of the reasons have to be emphasized:

Firstly, these machines differ from most common induction machines as the driven impeller is designed to be an integral part of the machine, rather than a separately driven component. While aluminium-made impeller is bolt on the shaft (or press-fitted) it is expected to play an important role in determining the temperature of the shaft, especially on its side, where it is attached to it.

As the impeller's prime function is creating partial vacuum and airflow for dust-pickup (when used in a vacuum cleaner), its complementary function is to ensure airflow through the motor. However, it is not always the same, but strongly dependent on the machine's operational point. In other words - as the vacuum cleaner dust bag is being filled up with trash and dust, increased flow resistance will result in less airflow through the motor. The motor will start to run hotter until the dust-bag is replaced with a new, empty one.

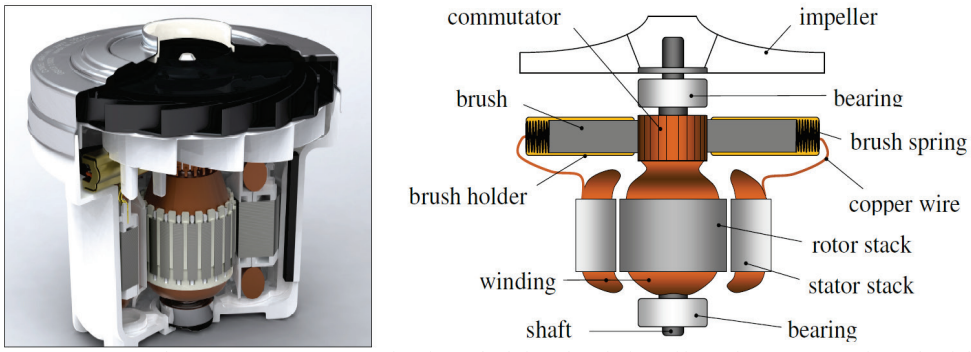

Figure 1 Vacuum cleaner motor; a cut-away view is on the left; a description of its main components is on the right

Secondly, most of the literature on thermal modelling of electric motors deals with totally enclosed, fan cooled (TEFC) motor design. There, heat exchange between the rotor, stator and frame is increased with forced air convection, caused by fan ventilation. Later on, heat is dissipated from the frame by means of forced or natural convection, meaning that the entire heat flux eventually has to go through motor's frame.

Contrary, the vacuum cleaner motor as a through-flow machine gives out heat into the environment mostly by means of constant delivery of cool (fresh) air, which intensifies the convection process due to large temperature difference.

Specific operational conditions in combinations with impeller integrated design and the particularities of cooling principles, are sufficiently important reasons to deal with thermal modelling of vacuum cleaner motor away from other types of induction motors.

To overcome mentioned obstacles and to estimate temperature changes within most vital motor components in a less time-consuming manner, there was increased need for development of a simplified thermal model for vacuum cleaner motor.

2 Lumped parameter network

Common electric motor temperature estimation methods can be divided into two basic types – analytical lumped-circuit and numerical methods. The numerical approach provides results very quickly, while developing thermal network usually demands some more effort to set the model, but requires less computational power [9]. Lumped parameter network has been used for different types of electric machines [1-7, 9, 10]. The method draws an analogy between thermal systems and electrical networks. It takes into account geometry, intrinsic thermal and physical properties of the system components and of the cooling circuit [11].

In the past decades the method, proposed by Mellor and Turner [6], was a reference method for many researchers working on induction motor thermal problems. Their lumped parameter model is based on subdividing the motor into several parts (called also lumps or elements) that are assumed to have constant temperature and similar thermal behaviour. The amount of energy flowing between adjacent elements depends on mutual thermal difference and interrelated thermal resistance between those elements. The accuracy of such a model mostly depends on the sufficient amount of elements, on correct estimation of the main thermal paths and on realistic assessment of thermal resistance between elements. If the network is correctly defined, it can offer fast and accurate temperature estimates. Furthermore, if the thermal node capacity of each element is known, such approach can be used also for dynamic thermal response modelling [12].

As already mentioned, most existing temperature estimation models are referred to as TEFC motors. The principles of modelling through flow universal motors (such as vacuum cleaner unit) remain similar, but in addition, fluid flow through the motor should be incorporated into the network. The proposed model for thermal analysis of induction machine with forced cooling channels was shown by Jokinen [13], who divides thermal network of the machine with coolant flow into four main parts:

- Forming thermal network of the machine
- Specifying thermal resistances
- Determination and distribution of losses
- Modelling coolant flow.

The vacuum cleaner motor with its main structural parts is shown in Fig. 1. The main considered thermal paths, loss origin and its distribution together with coolant flow can be visualized with thermal network, Fig. 2, where the main thermal paths are connected via resistances ($R_{i,j}$, with i^{th} and j^{th} node).

Loss positioning and its calculation is more precisely described in section 5, coolant modelling (nodes 24-27) under section 6.

3 Estimation of thermal resistances

To analyse the process of heat transfer in an electrical machine, a perfect machine geometry must be chosen and divided into lumped elements [14].

Following an example from ref. [14] also vacuum cleaner motor is considered as a combination of coaxial concentric cylinders (shaft, rotor iron, bearings) and cylindrical arc segments (teeth, slot), with the exception of stator pack. Nodes were placed on resistive midpoint of the element, as suggested by Andersson [15].

Due to a relatively small size of the motor elements thermal flow can be limited to only one dimension for some of the elements. To keep the model simpler, the following assumptions were made:

- no axial heat flux within the rotor pack and embedded parts of windings,

- only axial heat flux within the shaft elements, except its middle element (node 3), being in good contact with the rotor lamination,
- no heat flux in the circumferential direction within each element,
- uniform temperature of the stator lamination,
- neglected radiation, only conduction and convection.

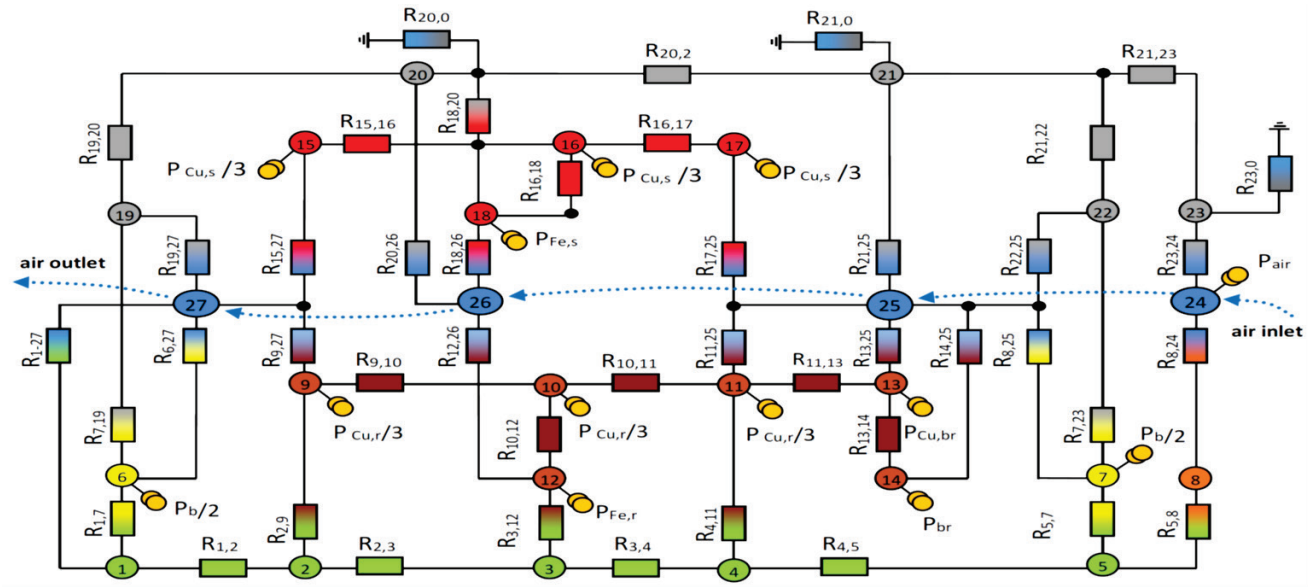

Figure 2 Thermal network of a vacuum cleaner unit: shaft elements (1-5) – green, bearings (6,7) – yellow, impeller (8) – orange, stator (15-18) – red, rotor (9-12) with commutator (13) and brush (14) – brown, frame (19-13) – grey, coolant (24-27) – blue.

Such assumptions are somewhat common for thermal modelling of electrical machines with lumped networks [1-7, 9, 10, 15].

3.1 Conduction

For the conduction mode, thermal resistances of arc segment elements depend on its geometry and material's thermal conductivity. Resistance is separately estimated for radial direction:

$$R_1 = \frac{1}{2 \cdot k_r \beta H}\left[\ln\frac{r_2}{r_1} - \frac{1}{2}\cdot(1-2B)\right], \quad (1)$$

$$R_2 = \frac{1}{2 \cdot k_r \beta H}[1-2B], \quad (2)$$

$$B = \frac{r_1^2}{r_2^2 - r_1^2}\cdot \ln\frac{r_2}{r_1}, \quad (3)$$

and for axial direction:

$$R_{1a} = R_{2a} = \frac{H}{2 \cdot k_a \cdot \beta \cdot (r_2^2 - r_1^2)}, \quad (4)$$

where r_1 and r_2 are the inner and outer diameter of the considered arc segment, β is its angle and H its length in axial direction. Coefficients k_r and k_a apply to the conductivity coefficient of the material in its radial and axial direction. By setting its inner diameter $r_1 \to 0$ for the shaft, corresponding resistances in its radial and axial direction can be simplified to:

$$R_{rr} = \frac{1}{4 \cdot k_r \beta H}, \quad (5)$$

$$R_o = \frac{H}{2 \cdot k_a \cdot \beta \cdot r_2^2}. \quad (6)$$

Similarly also thermal resistance in radial direction of the slot liner is modelled as an arc shaped strip, while slot windings are modelled as a rectangular slip, as in ref. [14].

3.2 Film coefficient

The film or convection coefficient being a function of many parameters makes convection complex to model. Material type, surface roughness, velocity of fluid and some of its characteristics (temperature, density, specific heat and dynamic viscosity) all significantly influence heat dissipation away from surfaces. Neglecting all these, in its simplest form heat removal can be expressed with a simple formula:

$$R_c = \frac{1}{h_c A}, \quad (7)$$

where h_c is the film coefficient, A surface of the element and R_c a given heat resistance.
As precise film coefficient is difficult to model, we decided to estimate its value separately for metal and plastic parts of our motor, where it is assumed:

- all metal parts have the same film coefficient $h_{c,met}$
- all other parts have the film coefficient $h_{c,pl}$

Coefficients $h_{c,pl}$ and $h_{c,met}$ are not known until the parameter tuning process is finished (see section 7).

While vacuum cleaner motor operates at different regime points (airflow, rotor speed), the relative surface speed of air varies significantly. Fortunately, the relation between air velocity and the film coefficient for highly developed turbulent flow ($Re > 3 \times 10^5$) is known to be approximately proportional to the square root of relative surface velocity v, Miller [16]:

$$h_c \propto v^{0,5} \quad (8)$$

To consider the influence of velocity, the so called speed coefficient is added to Eq. (8), resulting in:

$$R_{c,norm} = \frac{1}{h_c \cdot \left(\frac{v}{v_{\mathrm{norm}}}\right)^{0,5} \cdot A}, \tag{9}$$

where v_{norm} is normalized surface velocity (of 50m/s) and v actual relative surface velocity, which takes account of both – axial velocity v_a (caused by airflow) and radial velocity v_p (result of perpendicular speed of rotating part):

$$v = \sqrt{v_a^2 + v_p^2}. \tag{10}$$

Perpendicular velocity v_p is the product of mean surface radius r_m of the considered part and the rotor's angular speed ω. For stationary parts (stator parts, housing, bracket and cover) v_p is 0, except for the stator air-gap surface, where relative surface speed is assumed to be the same as relative velocity of rotor's lamination surface.

4 Loss estimation and distribution

Accurate prediction of temperature rise in electrical machines hinges on both correct equivalent network and correct allocation of losses [14].

The main power sources within the studied universal motor are resistive losses, iron core losses, frictional losses and aerodynamic losses, see Fig. 3.

4.1 Resistive losses

The main two sources are the stator and rotor winding coils, which can be apportioned between the slotted and end-winding regions. For commutator machines also brush to commutator contact losses and brush resistive losses should not be neglected [17, 18].

Due to thermally dependent electrical resistance, resistive ohm losses of stator $P_{\mathrm{Cu},s}(T)$ and rotor $P_{\mathrm{Cu},r}(T)$ at actual temperature (T) are estimated as:

$$P_{\mathrm{Cu,s}}(T) = I^2 \cdot R_{\mathrm{Cu},s}(T_0)[1 + \alpha_{Cu}(T - T_0)], \tag{11}$$
$$P_{\mathrm{Cu,r}}(T) = I^2 \cdot R_{\mathrm{Cu},r}(T_0)[1 + \alpha_{Cu}(T - T_0)], \tag{12}$$

where $R_{\mathrm{Cu},s}(T_0)$ corresponds to stator and $R_{\mathrm{Cu},r}(T_0)$ to rotor resistance measured at room temperature T_0,I is the electrical current of the motor, α_{Cu} is thermal coefficient of copper resistance.

Resistive losses of copper parts are corrected for the predicted temperatures iteratively with Matlab software. Similarly, resistive losses of carbon brushes can be calculated with ohm's law and additional transient current losses have to be articulated [19] as:

$$P_{\mathrm{br}} = I^2 \cdot R_{\mathrm{br}} + z \cdot I \cdot U_{\mathrm{tr}}, \tag{13}$$

where R_{br} is the resistance of brush, z is the number of sliding contacts and U_{tr} transient voltage drop per contact, usually of magnitude 1 V [19], as used for our model too. Thermal dependence of brushes is neglected due to its low (sometimes even negative) thermal coefficient. Resistive brush losses are assigned to brush node 14.

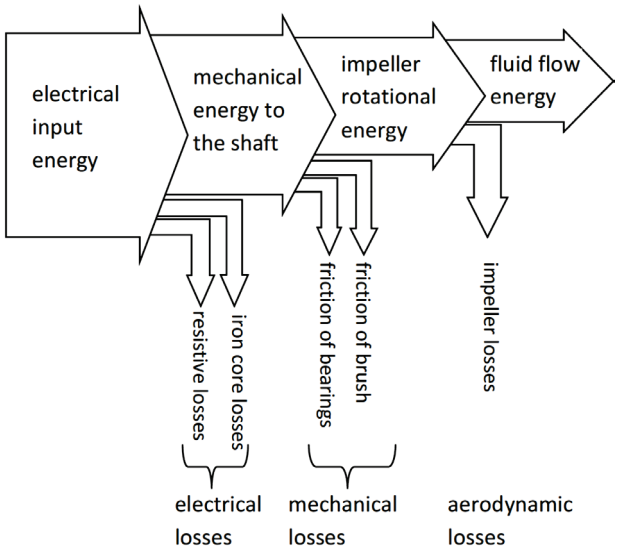

Figure 3 Energy-flow diagram for a vacuum cleaner motor

4.2 Iron core losses

Complete iron core losses P_{Fe} comprise hysteresis losses P_k and eddy-current losses P_e as:

$$P_k = k_h \cdot B^n \cdot f \cdot m_{\mathrm{Fe}}, \tag{14}$$
$$P_e = k_e \cdot B^n \cdot f^2 \cdot m_{\mathrm{Fe}}, \tag{15}$$

where k_h is eddy-current material constant and k_e hysteresis material constant at a given frequency (50 Hz), f is the actual frequency of alternating magnetic field, B maximum flux density, n is material dependent constant (between 1,6 and 2,0) and m_{Fe} is the mass of iron core. Magnetic flux density B is not constant over the whole lamination, so the mean value of B^n is estimated using FEM, as described by Benedičič [20] and used also in [21-23].

Iron losses are estimated and assigned separately for the rotor ($P_{\mathrm{Fe,r}}$) and the stator ($P_{\mathrm{Fe,s}}$) – to nodes 12 and 18.

4.3 Mechanical losses

The main sources of mechanical losses are estimated as a product of measured frictional moment M and rotor's angular velocity ω:

$$P_{\mathrm{b}}(n) = M_{\mathrm{b}} \cdot \omega, \tag{16}$$
$$P_{\mathrm{br}}(n) = M_{\mathrm{br}} \cdot \omega, \tag{17}$$

where M_{b} is the bearings frictional moment and M_{br} the brush frictional moment. They are experimentally determined in [8] as fitted polynomial functions of actual rotational speed of the machine.

4.4 Aerodynamic losses

A large proportion of aerodynamic losses originate in the polytrophic process within the impeller (and diffuser) thus named impeller losses P_{imp}. Those losses are assumed to appear directly in airflow as it goes through the impeller (node 24). They contribute to the temperature

rise of the cooling air, which in turn reduces the cooling efficiency of other components.

The amount of losses generated within the impeller is strongly related to the operational regime of the impeller. More specifically, for vacuum cleaner motor it means that impeller losses are the lowest near its optimum working point (q_{opt}), but when moving towards maximum airflow (q_{max}) or towards minimum airflow ($q_{\mathrm{min}} = 0$) impeller losses only increase. P_{imp} can be estimated as the difference between the input power P_{el} (electrical power of the motor) and the sum of other losses including air power P_{air}:

$$P_{\mathrm{imp}} = P_{\mathrm{el}} - P_{\mathrm{air}} - (P_{\mathrm{Fe}} + P_{\Omega} + P_{\mathrm{meh}}), \tag{18}$$

where complete iron losses P_{Fe} are the sum of $P_{\mathrm{Fe,r}}$ and $P_{\mathrm{Fe,s}}$, complete resistive losses P_{Ω} are the sum of $P_{\mathrm{Cu,r}}$, $P_{\mathrm{Cu,s}}$ and $P_{\Omega,\mathrm{br}}$ and complete mechanical losses P_{meh} are the sum of $P_{\mathrm{meh,br}}$ and $P_{\mathrm{meh,b}}$.

Working power P_{air} as the product of airflow q_{air} and generated pressure difference Δp is assumed to be translated into heat as air travels through its resistors (ducts, filters, dust bag, etc.):

$$P_{\mathrm{air}} = q_{\mathrm{air}} \cdot \Delta p, \tag{19}$$

Usually, the main flow resistors within vacuum cleaner (dust bag, tubes and filters) cause drag (resistance) of the flow before it even enters the motor. Therefore P_{air} is assumed to heat and enter the airflow before it enters the motor. Integration of P_{air} into coolant flow is described in the following section 5.

5 Modelling coolant flow

The simplest way to model coolant flow is to assume its constant temperature. Such approach gives adequately accurate results if the temperature rise of the coolant is small as it normally is in TEFC motors, where the same air circulates within the motor. However, for the vacuum cleaner motor, as a through-flow universal motor, such assumption is not adequate.

Jokinen [13] has shown how airflow equations, which assume gradual rise of the coolant, can be handled simultaneously with the thermal network of the machine – with the so-called "heat-flow controlled sources".

To simulate its gradual rise, coolant flow has several sequential zones (lumps). The division and number of selected nodes are based on the knowledge of the motor and its assumed airflow trajectory.

We assume that the coolant network of vacuum cleaner motor can be adequately described with 4 sequential zones – the impeller zone; the commutator zone, the air-gap zone and the outlet zone (nodes 24-27), see Fig. 2.

As cooling air is traveling through this node i its temperature rises for $\Delta\Theta_i$:

$$\Delta\Theta = \frac{\sum_{i=1}^{n} P_j}{\rho \cdot c_p \cdot q_{\mathrm{air}}} = 2R_q \cdot \left(\sum_{j=1}^{n} P_j\right), \tag{20}$$

where ρ is the density, c_p the specific heat capacity of the coolant, q_{air} the coolant flow, n the number of heat losses P entering the zone i and the term:

$$R_q = \frac{1}{2 \cdot \rho \cdot c_p \cdot q_{\mathrm{air}}}, \tag{21}$$

has the dimension of thermal resistance K/W, where mass flow $\rho \cdot c_p$ is not temperature dependent.

Temperature rise within each zone can be assumed as average temperature rise between inlet and outlet temperatures, Θ_{in} and Θ_{out}:

$$\Theta_{\mathrm{out}} = \Theta_{\mathrm{in}} + \frac{\Delta\Theta}{2} = R_q \cdot \left(\sum_{j=1}^{n} P_j\right). \tag{22}$$

In a matrix form, temperature rise of the coolant Θ for nodes 24-27 can be written as:

$$\begin{bmatrix} \Theta_{24} \\ \Theta_{25} \\ \Theta_{26} \\ \Theta_{27} \end{bmatrix} = \begin{bmatrix} R_q & 0 & 0 & 0 \\ 2R_q & R_q & 0 & 0 \\ 2R_q & 2R_q & R_q & 0 \\ 2R_q & 2R_q & 2R_q & R_q \end{bmatrix} \begin{bmatrix} \Phi_{8,24} + \Phi_{23,24} \\ \Phi_{7,25} + \Phi_{11,25} + \Phi_{13,25} + \Phi_{14,25} + \Phi_{17,25} + \Phi_{21,25} + \Phi_{22,25} \\ \Phi_{12,26} + \Phi_{18,26} + \Phi_{20,26} \\ \Phi_{1,27} + \Phi_{5,27} + \Phi_{6,27} + \Phi_{9,27} + \Phi_{15,27} + \Phi_{19,27} \end{bmatrix} + \begin{bmatrix} R_q \cdot P_{\mathrm{imp}} + 2R_q \cdot P_{\mathrm{air}} \\ 2R_q \cdot P_{\mathrm{imp}} + 2R_q \cdot P_{\mathrm{air}} \\ 2R_q \cdot P_{\mathrm{imp}} + 2R_q \cdot P_{\mathrm{air}} \\ 2R_q \cdot P_{\mathrm{imp}} + 2R_q \cdot P_{\mathrm{air}} \end{bmatrix}, \tag{23}$$

where $\Phi_{i,j}$ are unknown heat flows (from nodes i and j), P_{imp} are impeller losses (Eq. (18)) and P_{air} are air losses. In short form, Eq. (23) can be written as:

$$[\Theta_e] = [R_e] \cdot [\Phi_e] + [\Theta_\rho], \tag{24}$$

where $[\Theta_e]$ is the temperature rise vector, $[R_e] \cdot [\Phi_e]$ is the convection part (temperature rise caused by convection from machine elements) and $[\Theta_e]$ is the direct loss part (temperature rise caused by losses entering directly into coolant flow).

6 Solving equivalent circuit

Let's examine the solution of the equivalent circuit, Fig. 2, without a circuit analysis program. The machine has open-circuit cooling and there are 27 nodes in the circuit. The circuit equation of a short matrix form can be written as:

$$[G] \cdot [\Theta] = \begin{bmatrix} [P] \\ [-\Phi_e] \end{bmatrix}, \tag{25}$$

where $[G]$ is the conductance matrix:

$$[G]=\begin{bmatrix}\sum_{i=1}^{n}\frac{1}{R_{1,i}} & \frac{-1}{R_{1,2}} & \cdots & \frac{-1}{R_{1,n}}\\ \frac{-1}{R_{1,2}} & \sum_{i=1}^{n}\frac{1}{R_{2,i}} & \cdots & \frac{-1}{R_{2,n}}\\ \vdots & \vdots & \ddots & \vdots\\ \frac{-1}{R_{1,n}} & \frac{-1}{R_{2,n}} & \cdots & \sum_{i=1}^{n}\frac{1}{R_{n,i}}\end{bmatrix}, \tag{26}$$

$[P]$ is the loss vector concerning heat generation within machine parts

$$[P]=\begin{bmatrix}P_1\\P_2\\\vdots\\P_n\end{bmatrix}, \tag{27}$$

$[\theta]$is the unknown temperature vector:

$$[\theta]=\begin{bmatrix}\theta_1\\\theta_2\\\vdots\\\theta_m\end{bmatrix}, \tag{28}$$

$[\Phi_e]$ is the heat flow vector, as in Eqs. (23, 24). For Eqs. (26, 27) n is the number of solid part nodes (23), while index m is the number of all network nodes (27).

Combining Eqs. (24, 25), and following ref. [13] solution in a matrix form for the temperatures of all 27 nodes is with Eq. (29), which was solved with Matlab software.

$$[\Theta]=\left[[G]+\begin{bmatrix}0 & 0\\0 & [R_e]^{-1}\end{bmatrix}\right]^{-1}\left[\begin{matrix}[P]\\[R_e]^{-1}[\Theta_\rho]\end{matrix}\right]. \tag{29}$$

While thermal conductivity of copper, influencing winding losses $P_{\mathrm{Cu,r}}$ and $P_{\mathrm{Cu,s}}$– see Eqs. (11, 12), is temperature dependent, the final solution was achieved by means of Matlab reverse loop "while". Within the same loop, also impeller losses P_{imp} are iterativelly corrected, as their estimation depends on the estimation of other losses – Eq. (18).

7 Parameter tuning

Precise estimation of convection coefficients is a very complex process while the methods proposed by several authors [24] can yield significantly different results.

To overcome the complex process of heat transfer coefficients estimation, it is possible to combine the known heat transfer laws (domain knowledge – Eqs. (1)-(29) with the convection coefficient tuning process, Fig.4. Genetic algorithm was applied for coefficient tuning [25, 26].

The tuning process is based on finding film coefficients $h_{c,pl}$ and $h_{c,met}$ (see section 3.2) giving us a minimum difference between the measured and calculated temperature values, more specifically, minimum sum of its squared errors (SSE):

$$\Delta = SSE = \sum_i\left(\Theta(i)-\Theta_m(i)\right)^2, \tag{30}$$

where Θ_m applies for the measured temperatures and index i applies only for measurable node numbers ($i = 1,6,7,9,12,14-23$).

The tuning process yielded $h_{c,pl} = 242{,}9\ \mathrm{W/m^2K}$ and $h_{c,met} = 3270\ \mathrm{W/m^2K}$ giving $\Delta = 132\ \mathrm{K^2}$.

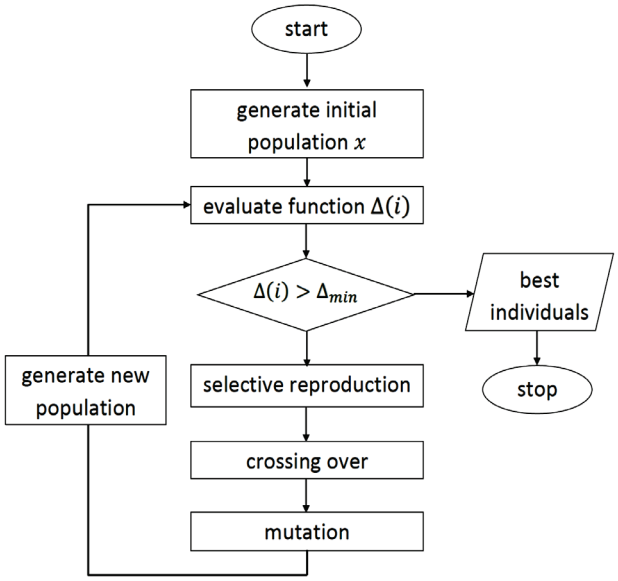

Figure 4 Block diagram of genetic algorithm (GA) evolutionary algorithm

8 Model verification

The results from the thermal model were cross checked against measurements made on two different motors (motor 1-1 kW and motor 2-2 kW). Motor 1 was used also for tuning the unknown film coefficients $h_{c,pl}$ and $h_{c,met}$, Fig. 5.

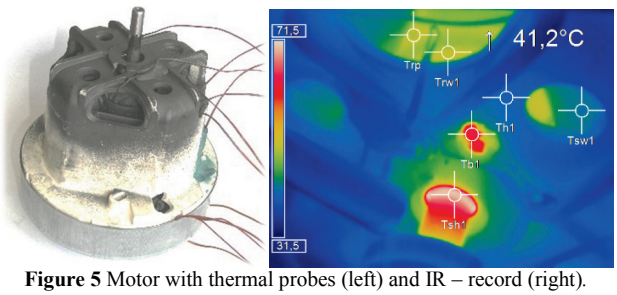

Figure 5 Motor with thermal probes (left) and IR – record (right).

To verify the robustness of the model, verification was performed not only on the same machine (no. 1) under different conditions, but also on another machine (no. 2) at two different sets of conditions, all together four different cases:

- Case 1 – machine 1, high airflow – learning example (tuning)
- Case 2 – machine 1, low airflow – verification of the model on the same machine as used for learning
- Case 3 – machine 2, high airflow – verification of how the model predicts temperature on another machine under similar conditions
- Case 4 – machine 2, low airflow – verification of how the model predicts temperature on another machine under a different regime point.

Tab. 1 shows that the model is able to correctly predict temperature not only for the machine that was used for tuning (cases 1 and 2), but also when used on another machine (cases 3 and 4) with significantly different design parameters and characteristics. The sum of squared errors as well as the mean absolute error is similar for all four selected cases. Mostly negative values of $\Theta_m - \Theta$ show that temperatures for much stronger machines are slightly underestimated, where the error is the greatest for rotor parts such as shafts, bearings, windings, brushes and rotor packs, followed by stator elements. Slight underestimation of temperatures on stronger machine (no. 2) is most probably the result of one of the model assumptions - constant thermal resistance of steel and iron parts, which is not exact. With temperatures above 100 °C thermal conductivity of irons and low alloy steels linearly decreases with rising temperature. Considering temperature dependency of thermal conductivity of metal parts would make the model even more robust, especially when used on powerful machines, which tend to heat more.

Table 1 Verification of results – Comparison between measured Θ_m and predicted Θ temperatures in °C

		case 1: tuning (learning example)			case 2: verification 1 (changed regime)			case 3: verification 2 (changed motor)			case 4: verification 3 (changed motor and regime)		
node	group	Θ_m	Θ	$\Theta-\Theta_m$	Θ_m	Θ	$\Theta-\Theta_m$	Θ_m	Θ	$\Theta-\Theta_m$	Θ_m	Θ	$\Theta-\Theta_m$
(1) shaft 1 – outlet side	shaft	45,2	49,0	3,8	60,0	64,3	4,3	92,3	85,9	−6,4	122,8	117,4	−5,4
(2) shaft 2		*	47,7	*	*	61,2	*	*	89,7	*	*	114,2	*
(3) shaft 3		*	46,4	*	*	60,0	*	*	86,5	*	*	113,1	*
(4) shaft 4		*	46,0	*	*	58,1	*	*	85,4	*	*	112,9	*
(5) shaft 5 – inlet side		*	45,2	*	*	60,2	*	*	84,8	*	*	112,9	*
(6) bearing – outlet side	bearings	42,8	44,2	1,4	60,3	63,9	3,5	84,3	79,2	−5,1	113,6	107,1	−6,4
(7) bearing – inlet side		40,5	42,7	2,2	58,6	57,2	−1,4	78,2	74,8	−4,4	95,1	90,3	−4,8
(8) impeller	impeller	*	38,6	*	*	49,4	*	*	49,6	*	*	65,3	*
(9) rotor end w. – outlet side	rotor	76,1	79,0	2,9	98,8	97,9	−0,9	130,0	130,4	−3,4	148,8	143,1	−5,7
(10) rotor embedded winding		*	65,3	*	*	85,6	*	*	112,6	*	*	122,4	*
(11) rotor end w. – inlet side		*	76,3	*	*	92,4	*	*	126,3	*	*	138,6	*
(12) rotor pack		59,8	61,9	2,1	82,2	79,5	−2,7	107,0	102,8	−4,2	119,2	114,9	−4,3
(13) commutator	brush	*	43,7	*	*	71,3	*	*	76,0	*	*	105,0	*
(14) brush		46,3	44,5	−1,8	74,4	72,6	−1,8	80,5	78,2	−3,3	105,7	101,7	−4,0
(15) stator end w. – outlet side	stator	64,5	68,3	3,8	96,5	100,8	4,2	147,1	144,1	−3,1	148,3	146,8	−1,5
(16) stator embedded winding		55,0	58,3	3,3	80,0	83,6	3,6	102,2	98,6	−3,6	113,3	112,0	−1,3
(17) stator end w. – inlet side		60,7	63,0	2,3	85,8	88,4	2,6	138,0	134,6	−3,4	143,7	140,0	−3,7
(18) stator pack		40,0	44,3	4,3	60,0	63,7	3,7	66,5	66,1	−0,4	88,9	86,5	−2,4
(19) housing – outlet side	frame	34,2	37,6	3,4	49,3	54,0	4,7	48,5	47,6	−0,9	64,2	63,7	−0,5
(20) housing – middle		35,3	32,0	−3,3	48,5	46,6	−1,9	52,3	50,2	−2,1	63,7	65,5	1,8
(21) housing – inlet side		39,3	35,5	−3,8	57,6	55,5	−2,1	61,6	59,4	−2,2	80,9	82,9	2,0
(22) bracket		39,5	36,9	−2,6	59,9	58,2	−1,7	63,0	61,3	−1,7	82,3	83,3	1,0
(23) cover		35,1	33,6	−1,5	48,7	48,8	0,1	50,7	47,6	−3,1	63,5	61,7	−1,8
sum of squared errors – Δ (°C)		132,0			128,5			182,2			195,7		
mean absolute error (°C)		**2,8**			**2,6**			**3,1**			**3,1**		

9 Conclusions

The lumped thermal model for a vacuum cleaner motor as an open-circuit cooling machine has been developed, discussed and successfully verified. The model is based on dimensional data, physical and thermal constants and experimental heat transfer characteristics, used for the tuning of unknown film coefficients.

Simulation results from the proposed thermal model are in good agreement with the measurements, conducted on test bench, allowing the estimation of temperature for different motor parts (windings, bearings, brush and housing) and for different operational points of the motor.

Additional improvement of the model can be made in terms of its increased robustness. As already discussed under section 8, the model could improve its prediction accuracy if thermal conductivity of metals (shaft, iron lamination) were considered as the linear function of temperature.

The thermal model will be in the next step used for the research on the correlation between bearings temperature and their life span. The bearings temperature will be by means of the model determined on the basis of the motor and operating parameters. This will enable data mining of several hundred of bearing life span tests conducted in the last years.

Acknowledgements

The authors kindly acknowledge the European Social Fund and the Slovenian Ministry of Higher Education, Science and Technology for financially supporting this research. The authors would also like to thank the Domel d.o.o. company and its directors for their collaboration and approval to publish this work.

10 References

[1] Bellenda, G.; Ferraris, L.; Tenconi, A. A new simplified thermal model for induction motors for EVs applications. // Electrical Machines and Drives, 1995. Seventh International Conference on (Conf. Publ. No. 412), 1995, pp. 11-15.

[2] Boglietti, A.; Cavagnino, A.; Popescu, M.; Staton, D. Thermal Model and Analysis of Wound-Rotor Induction Machine. // Industry Applications, IEEE Transactions on. 49, (2013), pp. 2078-2085. DOI: 10.1109/TIA.2013.2261444

[3] Chowdhury, S. K.; Baski, P. K. A simple lumped parameter thermal model for electrical machine of TEFC design. // Power Electronics, Drives and Energy Systems (PEDES) & 2010 Power India, 2010 Joint International Conference on, 2010, pp. 1-7.

[4] Duran, M. J.; Fernandez, J. Lumped-parameter thermal model for induction machines. // Energy Conversion, IEEE Transactions on. 19, (2004), pp. 791-792. DOI: 10.1109/TEC.2004.837272

[5] Kral, C.; Haumer, A.; Sang Bin, L. Robust thermal model for the estimation of rotor cage and stator winding temperatures of induction machines. // Electrical Machines (ICEM), 2012 XXth International Conference on, 2012, pp. 1810-1816.

[6] Mellor, P. H.; Roberts, D.; Turner, D. R. Lumped parameter thermal-model for electrical machines of TEFC design. // IEE Proceedings-B Electric Power Applications. 138, (1991), pp. 205-218.

[7] Nategh, S.; Huang, Z.; Krings, A.; Wallmark, O.; Leksell, M. Thermal Modeling of Directly Cooled Electric Machines Using Lumped Parameter and Limited CFD Analysis. // IEEE Transactions on Energy Conversion. 28, (2013), pp. 979-990. DOI: 10.1109/TEC.2013.2283089

[8] Benedik, B.; Tavčar, J.; Duhovnik, J. Thermal model of a vacuum cleaner unit developed with application of regression method. // Tools and methods of competitive engineering, University of Technology, Delft, 2014, pp. 819-830.

[9] Boglietti, A.; Cavagnino, A.; Staton, D.; Shanel, M.; Mueller, M.; Mejuto, C. Evolution and Modern Approaches for Thermal Analysis of Electrical Machines. // Industrial Electronics, IEEE Transactions on. 56, (2009), pp. 871-882. DOI: 10.1109/TIE.2008.2011622

[10] Yunkai, H.; Jianguo, Z.; Youguang, G. Thermal Analysis of High-Speed SMC Motor Based on Thermal Network and 3-D FEA with Rotational Core Loss Included. // Magnetics, IEEE Transactions on. 45, (2009), pp. 4680-4683. DOI: 10.1109/TMAG.2009.2023065

[11] Bertin, Y.; Videcoq, E.; Thieblin, S.; Petit, D. Thermal behavior of an electrical motor through a reduced model. // Energy Conversion, IEEE Transactions on. 15, (2000), pp. 129-134. DOI: 10.1109/60.866989

[12] Mellor, P. H.; Turner, D. R. Real Time Prediction of Temperatures in an Induction Motor Using a Microprocessor. // Electric Machines & Power Systems. 15, (1988), pp. 333-352. DOI: 10.1080/07313568808909342

[13] Jokinen, T.; Saari, J. Modelling of the coolant flow with heat flow controlled temperature sources in thermal networks. // IEE Proceedings - Electric Power Applications. 144, (1997), pp. 338-342. DOI: 10.1049/ip-epa:19971384

[14] Bousbaine, A. Thermal Modelling of Induction Motors Based on Accurate Loss Density Distribution. // Electric Machines & Power Systems. 27, (1999), pp. 311-324. DOI: 10.1080/073135699269325

[15] Andersson, B. Lumped Parameter Thermal Modelling of Electric Machines. // Analysis of an Interior Permanent Magnet Synchronous, Machine for Vehicle Applications, Master of Science thesis, Chalmers university of technology, Goteborg, Sweden, (2013).

[16] Miller, T. Switched Reluctance Motor and Their Control, Magna Physics and Clarendon Press. Oxford, 1993.

[17] Pyrhönen, J.; Jokinen, T.; Hrabovcová, V. Design of rotating electrical machines. Wiley, Chichester, 2014.

[18] Bradley, K. J. Thermal modelling of AC commutator motors for domestic appliances. // Thermal Aspects of Machines, IEE Colloquium on. (1992), pp. 2/1-2/2.

[19] Miljavec, D.; Jereb, P. Električni stroji: temeljna znanja. Fakulteta za elektrotehniko, 2008.

[20] Benedičič, B. Model komutacije univerzalnega komutatorskega motorja // doctoral dissertation, Ljubljana, 2004, pp. II, 148.

[21] Korousic-Seljak, B.; Papa, G.; Benedicic, B.; Kmecl, T. Improving the technical quality of a universal motor using an evolutionary approach. // Proceedings of Euromicro Conference 2001, 27th, 2001, pp. 287-293. DOI: 10.1109/eurmic.2001.952466

[22] Benedičič, B.; Kmecl, T.; Papa, G.; Korousic-Seljak, B. Evolutionary optimization of a universal motor. // Industrial Electronics Society, 2001. IECON '01. The 27th Annual Conference of the IEEE, 2001, vol. 11, pp. 19-24.

[23] Papa, G.; Korousic-Seljak, B.; Benedicic, B.; Kmecl, T. Universal motor efficiency improvement using evolutionary optimization. // Industrial Electronics, IEEE Transactions on. 50, (2003), pp. 602-611. DOI: 10.1109/TIE.2003.812455

[24] Staton, D. A.; Cavagnino, A. Convection Heat Transfer and Flow Calculations Suitable for Electric Machines Thermal Models. // Industrial Electronics, IEEE Transactions on. 55, (2008), pp. 3509-3516. DOI: 10.1109/TIE.2008.922604

[25] Slak, A.; Tavčar, J.; Duhovnik, J. Dynamic planning and multicriteria scheduling of turned parts' production. // Tehnički vjesnik - Techincal Gazette. 17, 4(2010), pp. 453-464.

[26] Ji, W.; Wang, J.; Zhang, J. An improved real hybrid genetic algorithm. // Tehnicki vjesnik-Technical Gazette. 21, 5(2014), pp. 979-986.

Authors' addresses

Blaž Benedik, Ph.D. student
Domel, EMs and Home Appliances, d.o.o.,
Otoki 21, SI-4228 Železniki, Slovenia
E-mail: blaz.benedik@domel.si

Jože Duhovnik, Professor
Laboratory for Engineering Design,
Faculty of Mechanical Engineering, University of Ljubljana,
Aškerčeva 6, SI-1000 Ljubljana, Slovenia
E-mail: joze.duhovnik@lecad.fs.uni-lj.si

Janez Rihtaršič, Ph.D.
Domel, EMs and Home Appliances, d.o.o.,
Otoki 21, SI-4228 Železniki, Slovenia
E-mail: janez.rihtarsic@domel.si

Jože Tavčar, Professor
Laboratory for Engineering Design,
Faculty of Mechanical Engineering, University of Ljubljana,
Aškerčeva 6, SI-1000 Ljubljana, Slovenia
E-mail: joze.tavcar@lecad.fs.uni-lj.si